LA-4480-MS

LOS ALAMOS SCIENTIFIC LABORATORY
of the
University of California
LOS ALAMOS • NEW MEXICO

CMF-13 Research on Carbon and Graphite

Report No. 13

Summary of Progress from February 1 to April 30, 1970

This LA. . .MS report presents the summary of progress of CMF-13 research
on carbon and graphite at LASL. Previous summary of progress reports in this
series, all unclassified, are:

LA-3693-MS	LA-3932-MS	LA-4171-MS
LA-3758-MS	LA-3989-MS	LA-4237-MS
LA-3821-MS	LA-4057-MS	LA-4333-MS
LA-3872-MS	LA-4128-MS	LA-4417-MS

This report, like other special-purpose documents in the LA. . .MS series, has
not been reviewed or verified for accuracy in the interest of prompt distribution.

LOS ALAMOS SCIENTIFIC LABORATORY
of the
University of California
LOS ALAMOS • NEW MEXICO

CMF-13 Research on Carbon and Graphite

Report No. 13

Summary of Progress from February 1 to April 30, 1970*

by

Morton C. Smith

CMF-13 RESEARCH ON CARBON AND GRAPHITE

REPORT NO. 13: SUMMARY OF PROGRESS FROM FEBRUARY 1 TO APRIL 30, 1970

by

Morton C. Smith

I. INTRODUCTION

This is the thirteenth in a series of progress reports devoted to carbon and graphite research in LASL Group CMF-13, and summarizes work done during the months of February, March, and April, 1970. It should be understood that in such a progress report many of the data are preliminary, incomplete, and subject to correction, and many of the opinions and conclusions are tentative and subject to change. This report is intended only to provide up-to-date background information to those who are interested in the materials and programs described in it, and should not be quoted or used as reference publicly or in print.

Research and development on carbon and graphite were undertaken by CMF-13 primarily to increase understanding of their properties and behavior as engineering materials, to improve the raw materials and processes used in their manufacture, and to learn how to produce them with consistent, predictable, useful combinations of properties. The approach taken is microstructural, based on study and characterization of natural, commercial, and experimental carbons and graphites by such techniques as x-ray diffraction, electron and optical microscopy, and porosimetry. Physical and mechanical properties are measured as functions of formulation, treatment, and environmental variables, and correlations are sought among properties and structures. Raw materials and manufacturing techniques are investigated, improved, and varied systematically in an effort to create specific internal structures believed to be responsible for

desirable combinations of properties. Prompt feedback of information among these activities then makes possible progress in all of them toward their common goal of understanding and improving manufactured carbons and graphites.

Since its beginning, this research has been sponsored by the Division of Space Nuclear Systems of the United States Atomic Energy Commission, through the Space Nuclear Propulsion Office. More recently additional general support for it has been provided by the Office of Advanced Research and Technology of the National Aeronautics and Space Administration. Many of its facilities and services have been furnished by the Division of Military Application of AEC. The direct and indirect support and the guidance and encouragement of these agencies of the United States Government are gratefully acknowledged.

II. SANTA MARIA COKE

A. Previous Work

CMF-13 investigations of Santa Maria petroleum coke and of graphites made from it have previously been summarized in the ninth, tenth, eleventh, and twelfth reports in this series.

B. Grinding (R. J. Imprescia)

Specimen 63J-2, described on page 13 of Report No. 12, cracked into two pieces during the hot-molding cycle. Test bars machined from these pieces demonstrated that-- aside from its tendency to crack--this graphite had unusu-

TABLE I

SCREEN ANALYSES OF GRINDING PRODUCTS

CMF-13 Lot No.	Grind	Feed Rate, g/min		Weight Percent in Screen Fraction						
		1st Pass[a]	2nd Pass[b]	+16	-16+25	-25+45	-45+80	-80+170	-170+325	-325
CL-9	---	---	---	58.3	20.2	15.6	3.9	1.2	0.3	0.5
CP-8(900)b	---	---	---	0	0	5.3	29.2	28.9	16.5	20.1
---	S	90	---	4.5	4.5	31.0	26.5	15.5	9.0	9.0
---	S+1	90	10	0	0	Tr	13.0	34.0	27.5	25.5
---	S+2	90	20	0	0	Tr	15.0	35.0	25.0	25.0
---	S+3	90	30	0	0	Tr	15.5	35.0	25.0	24.5
---	S+4	90	40	0	0	Tr	12.5	33.0	25.5	29.0
---	S+5	90	50	0	0	Tr	14.0	32.5	26.0	27.5
---	S+6	90	70	0	0	Tr	15.5	32.5	21.0	31.0
---	S+7	90	90[c]	0	0	0	16.0	34.0	20.5	29.5
---	1A	147	---	5.5	7.0	27.5	27.0	15.5	7.5	10.0
---	1B	290	---	4.0	4.5	33.0	23.5	18.0	5.0	12.0
---	1D	374	---	2.5	5.5	30.5	28.0	13.5	7.5	12.5
---	1C	462	---	3.0	8.0	29.0	27.5	15.0	6.5	11.0
CP-16	W	350	---	1.5	7.0	28.5	28.0	13.5	9.5	12.0
---	W+1	350	80	0	0	2.5	21.5	34.0	22.0	19.5
---	W+2	350	100	0	0	2.0	16.0	34.0	20.0	28.0
---	W+3	350	120	0	0	1.0	15.5	33.5	17.5	32.5
---	W+4	350	145[c]	0	0	1.0	16.0	31.5	20.5	31.5
CP-17	W+2	350	100	0	Tr	6.8	20.0	31.0	17.2	25.0

(a) Williams mill with 1/8-in. dia discharge screen.

(b) Weber mill with 0.040-in. dia discharge screen.

(c) Discharge screen began to deform at this feed rate.

ally attractive properties. Unfortunately, only a small amount of the filler used to make 63J-2 was produced, and this was nearly exhausted in making the 63J series of graphites. An attempt has therefore been made to prepare another filler which behaves similarly, to be used in efforts to reproduce or improve upon the properties of 63J-2 and if possible to reduce its cracking tendency.

The filler used to make 63J-2 was CMF-13 Lot CP-8 (900)b, produced by vacuum-calcining green Santa Maria coke at 900°C and then grinding it in two stages of hammer milling. (The characteristics of this filler are listed in detail on page 9 of Report No. 12, and its screen analysis in Table I of this report. To avoid the calcination treatment, the starting material used for this new series of tests was Santa Maria LV coke, CMF-13 Lot CL-9, which had been calcined by its manufacturer at perhaps 1100°C. This is a lump coke with a maximum particle diameter of about 3/8 in. Its screen analysis is given in Table I. To minimize grinding time, only hammer milling was to be used, with as few grinding passes as possible.

In the first set of grinding experiments, a relatively large sample of Lot CL-9 lump coke was given a coarse
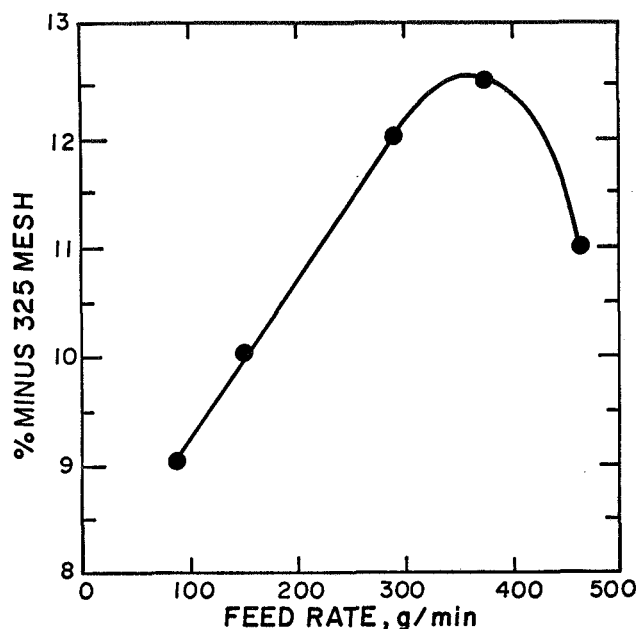
Fig. 1. Effect of feed rate to the Williams hammer mill on the proportion of minus 325 mesh fines produced in grinding Lot CL-9, Santa Maria LV coke.

Fig. 2. Effect of feed rate to the Weber hammer mill on the proportion of minus 325 mesh fines produced in grinding Lot CP-16 coke.

grind in the Williams hammer mill using the conditions of grind S (1/8-in. discharge screen, 90 g/min). The product was divided into seven smaller samples, which were ground individually in the Weber hammer mill using a 0.040-in. discharge screen and feed rates ranging from 10 to 90 g/min. Screen analyses of the Weber-mill products are given in Table I as grinds S+1, S+2, etc. All are much finer than CP-8(900)b, and no systematic variation of fineness with feed rate to the mill was apparent.

Grind S produces a product so coarse that, when it is fed to the Weber mill at high rates, it tends to damage the discharge screen of the Weber mill. Therefore four additional grinds were made in the Williams mill under the conditions of grind S except that feed rate was increased in steps up to 462 g/min. Feed rates and screen analyses of the grinding products, identified as grinds 1A, 1B, 1C, and 1D, are listed in Table I. As is frequently true, the curve of percent minus 325 mesh material in the product vs feed rate, plotted in Fig. 1, passed through a maximum, estimated in this case to occur at a feed rate of 350 g/min. Since a relatively fine feed was desired for second-stage grinding in the Weber mill, a 50 lb lot of CL-9
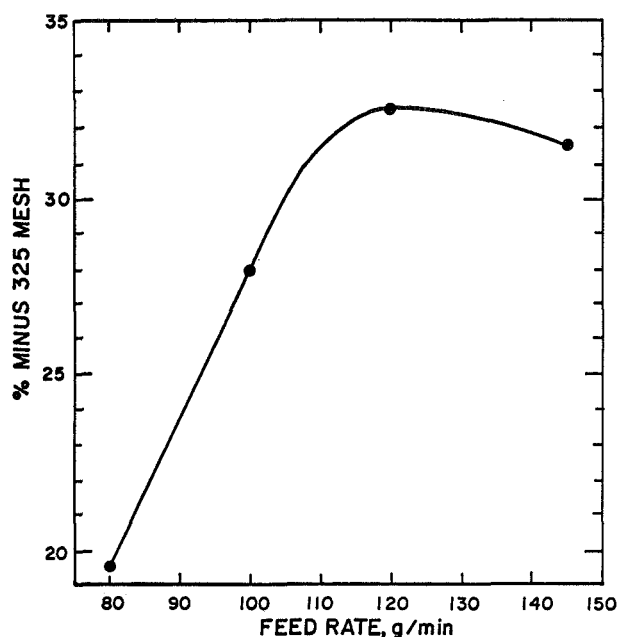
coke was ground under these conditions in the Williams hammer mill. (These conditions, now identified as "grind W", are use of a discharge screen with 1/8-in. dia holes and a feed rate of 350 g/min.) Screen analysis of the product, identified as CMF-13 Lot No. CP-16, is listed in Table I. As would be expected, it is similar to grind 1D.

Using Lot CP-16 as feed to the Weber mill, equipped with a discharge screen containing 0.040-in. dia holes, four second-pass grinds were made at feed rates of 80 to 145 g/min. Screen analyses of the grinding products (identified is grinds W+1, W+2, W+3, and W+4) are listed in Table I, the proportion of minus 325 mesh material in each is plotted as a function of feed rate to the mill in Fig. 2, and other particle characteristics are summarized in Table II. The use of grind W in the Williams mill as the first grinding pass was successful in increasing the allowable feed rate to the Weber mill. The curve of Fig. 2 again shows a maximum, in this case at a feed rate of about 120 g/min, and demonstrates the possibility of controlling fineness of the product over quite a broad range by varying the feed rate to the Weber mill. Presumably

3

TABLE II

PARTICLE CHARACTERISTICS OF GRINDING PRODUCTS

	Grind W + 1	Grind W + 2	Grind W + 3	Grind W + 4	Lot CP-17
Helium Pycnometer Density, g/cm^3	1.870	1.879	1.884	1.889	1.871
Standard Deviation	0.004	0.001	0.001	0.001	0.001
Micromerograph Sample Statistics					
Lognormal Model					
$\hat{\mu}_{x3}$	4.644	4.236	4.350	4.478	4.574
$\hat{\sigma}_x^2$	1.822	1.988	1.952	2.439	2.060
$\hat{\mu}_x$	-0.821	-1.728	-1.505	-2.838	-1.607
$\hat{\mu}_{d_3}$, microns	258.43	186.70	205.70	298.20	271.50
$\hat{\mu}_d$, microns	1.094	0.480	0.589	0.198	0.562
$\hat{\sigma}_d^2$, microns^2	6.198	1.452	2.097	0.411	2.161
S_W, cm^2/g	767.6	1247.7	1092.5	1220.1	927.4
CV_d	2.28	2.51	2.46	3.23	2.62
Interval Model					
$\bar{x}_3$	4.441	4.164	4.151	4.132	4.382
s_x^2	0.259	0.434	0.216	0.141	0.261
$\bar{x}$	0.185	0.442	0.235	0.080	0.404
$\bar{d}_3$, microns	130.17	103.26	100.15	98.06	134.85
$\bar{d}$, microns	1.478	2.091	1.490	1.220	1.787
s_d^2, microns^2	3.507	6.990	2.535	1.291	3.520
S_W, cm^2/g	897	1082	1270	1506	1067
CV_d	1.27	1.26	1.07	0.92	1.05
Surface-Area Data, BET Analysis					
$\bar{S}_W$, cm^2/g	51,460	66,890	73,230	74,790	62,600
Standard Deviation	1300	1800	4300	1600	200
d_s, micron	0.624	0.477	0.436	0.425	0.512
Fuzziness Ratio					
Lognormal Model	67.00	53.61	67.03	61.30	67.53
Interval Model	57.37	61.82	57.66	49.66	58.67

because the grinding characteristics of Santa Maria coke are strongly affected by the temperature to which it has been calcined, none of these products of grinding the LV coke closely approximated Lot CP-8(900)b. However, grinds W+1 and W+2, in particular, resembled that lot closely enough to be of interest for use as fillers in making graphites like 63J-2. Molded graphites have been made from all four grinding products, and are discussed below.

The Micromerograph analyses were made by H. D. Lewis, CMF-13, on the minus 50 mesh screen fractions of the various grinding products, and then corrected for presence of the plus 50 mesh material to give the results listed in Table II. Log-probability plots of the Micromerograph data showed that, as is common among Santa Maria fillers, each of these products was deficient in material

TABLE III

DENSITIES AND SHRINKAGES OF HOT-MOLDED GRAPHITES MADE FROM SANTA MARIA FILLERS

Speci-men No.	Mix Comp., pph Filler Identi-fication	Pitch Bin-der[a]	Molding Pressure, psi	Bulk Density, g/cm^3 Baked	Graph.	Dimensional Change, Baked to Graph., % Δl	Δd	Δv	Appearance
63J-2	CP-8(900)b	30	4000	1.74	1.80	-3.6	-3.2	-9.6	Cracked diametrally
63Jb-1	CP-8(900)b	30	4000	1.74	1.80	-3.7	-3.4	-10.2	Cracked diametrally
63Jb-2	CP-8(900)b	30	2000	1.74	1.81	-4.0	-3.6	-10.9	Cracked radially
63Jb-3	CP-8(900)b	30	1000	1.73	1.82	-4.3	-4.3	-12.3	Cracked radially
63Jb-4	CP-8(900)b	30	500	1.72	1.84	-4.7	-4.3	-12.6	Sound
63J-3	CP-8(900)b	30	250	1.65	1.73	-3.9	-3.6	-10.1	Sound
64F-1	S+6	30[b]	4000	1.62	1.73	-4.2	-3.9	---	Cracked
64E-1	S+10[c]	42.9[b]	4000	1.55	1.62	-4.6	-2.9	---	Sound
64G-1	W+1	30	4000	1.69	1.79	-3.9	-3.8	---	Sound
64H-1	W+2	30	4000	1.68	1.80	-4.3	-4.0	-11.7	Sound
64H-3	W+2	30	2000	1.66	1.77	-4.2	-3.9	-11.5	Sound
64H-2	W+2	30	500	1.66	1.65	0	0	0	Sound
64I-1	W+3	30	4000	1.67	1.77	-4.0	-3.8	---	Sound
64J-1	W+4	30	4000	1.66	1.76	-3.9	-3.7	---	Sound

(a) Barrett 30MH coal-tar pitch except where noted.

(b) Barrett 23S coal-tar pitch.

(c) Prepared by following the S grind with a second pass through the Williams mill using a

1/16-in. dia screen and a feed rate of 114 g/min.

in the particle size range about 20 to 60 μ dia, which was compensated by extra material in the size range below about 10 μ dia. As a result, the size distributions are poorly represented by the lognormal approximation, and the lognormal statistics of Table II are listed simply for comparison with data previously given on this basis. Statistics derived from use of the interval model are obviously more representative of these grinding products, and of Santa Maria fillers in general.

A 40-lb lot of filler material has since been prepared for future experiments by grinding the lump Santa Maria LV coke (CMF-13 Lot CL-9) using the W+2 grinding schedule. This grinding product, now identified as Lot CP-17, is slightly coarser than the original "W+2" lot, but is quite similar to it in screen analysis and other particle

characteristics. The two are compared in Tables I and II.

C. Molded Graphites (R. J. Imprescia)

1. Series 63J: Enough of the CP-8(900)b Santa Maria coke filler was still on hand to permit manufacture of a few molded specimens in order to examine the cracking behavior of graphites similar to 63J-2. A new mix was prepared from this filler using the same binder (30 pph of Barrett 30MH coal-tar pitch) and mixing procedures used to make 63J-2. These graphites, the 63Jb series, are listed in Table III. All were graphitized in flowing helium to 2800°C.

Specimen 63Jb-1 was hot-molded in a 2.75-in. dia die using the same conditions previously used to produce 63J-2

TABLE IV

PROPERTIES OF HOT-MOLDED GRAPHITES MADE FROM SANTA MARIA FILLERS

Specimen No.	63J-2[c]	63Jb-1[c]	63Jb-2[c]	63Jb-3[c]	63Jb-4	63J-3	64F-1[c]	64E-1	64G-1	64H-1
Density, g/cm^3	1.80	1.80	1.81	1.82	1.84	1.73	1.73	1.62	1.79	1.80
Tensile Str., psi										
With-grain	4130	---	2702	2076	1669	2616	2092[d]	1502	3683[d]	3484[d]
Compr. Str., psi										
With-grain	15,580	---	---	---	---	---	---	---	---	---
Across-grain	16,230	---	---	---	---	---	---	---	---	---
Flexure Str., psi										
With-grain	5854	2130	4135	3650	4313	4352	3891	2131	5737	5759
Across-grain	6773	930	3338	2436	1904	3475	4109	2042	6014	5892
Young's Mod., 10^6 psi										
With-grain	1.41	---	---	---	---	---	---	---	---	---
Across-grain	1.47	---	---	---	---	---	---	---	---	---
CTE, x 10^{-6}/°C[a]										
With-grain	5.56	5.31	5.03	5.08	5.13	5.70	5.68	5.00	---	---
Across-grain	5.69	5.84	5.02	5.56	5.47	5.50	5.92	5.58	---	---
Therm. Cond., W/cm-°C										
With-grain	1.10	1.10	1.06	1.04	1.01	1.10	0.96	0.86	1.10	1.10
Across-grain	1.06	0.79	1.03	1.04	0.94	0.95	0.92	0.76	1.06	1.10
Resistivity, μΩcm										
With-grain	1246	1488	1272	1242	1525	1552	1567	1823	1285	1285
Across-grain	1223	1619	1463	1368	1426	1483	1407	2043	1261	1290
Anisotropies										
BAF[b]	1.023	1.026	1.018	~1.00	1.033	1.012	1.018	1.018	1.006	1.022
Compr. Str.	1.04	---	---	---	---	---	---	---	---	---
Flexure Str.	0.86	2.29	1.24	1.50	2.27	1.25	0.95	1.04	0.95	0.98
Young's Mod.	0.96	---	---	---	---	---	---	---	---	---
CTE	1.02	1.10	1.00	1.09	1.07	0.96	1.04	1.12	---	---
Therm. Cond.	1.04	1.39	1.03	1.00	1.07	1.16	1.04	1.13	1.04	1.00
Resistivity	0.98	1.09	1.15	1.10	0.94	0.96	0.90	1.12	0.98	1.00

(a) Coefficient of thermal expansion, average, 25-645°C.

(b) Bacon anisotropy factor, σ_{oz}/σ_{ox}.

(c) Specimen cracked during molding.

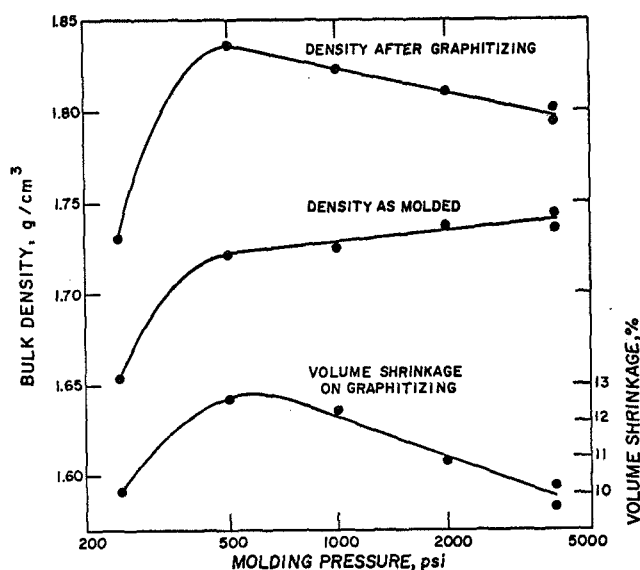(d) Broke in threads during tensile test.

Fig. 3. Effect of molding pressure on bulk densities and volume shrinkage during graphitization, 63J graphites.

(molding cycle "A", 4000 psi). Like 63J-2, it was found when removed from the die to have cracked diametrally into two almost equal pieces. Densities and shrinkages were also similar to those of 63J-2. However, as is shown in Table IV, its other properties were inferior to those of 63J-2, and it was quite anisotropic. This is evidently the result of the presence in 63Jb-1 of a large number of oriented defects, probably microcracks normal to the molding direction.

Specimens 63Jb-2 and 63Jb-3 were molded at 4-in. dia under pressures of 2000 and 1000 psi respectively but with the same temperature cycle used for 63J-2. As removed from the die both were cracked radially into three unequal, pie-shaped segments. Baked densities were slightly lower than when the normal modling pressure (4000 psi) was used, but this was more than compensated by increased shrinkage during graphitization. As a result, graphitized bulk density actually increased as molding pressure was reduced. This trend continued for specimen 63Jb-4, which was molded at 500 psi and which appeared to be sound when removed from the die. A further reduction of molding pressure to 250 psi for specimen 63J-3 reduced both the baked and the graphitized densities. As is illustrated by Fig. 3, at least for this particular filler

material, there is a specific, rather low molding pressure which results in maximum volume shrinkage during graphitization and maximum bulk density after graphitization. It is not clear why shrinkage is reduced when molding pressures are higher than this. However, it seems unlikely that this general effect would occur if the filler were graphitized or even calcined to a temperature high enough so that its shrinkage during graphitization was small.

The densities of this group of graphites did not correlate with their other properties. The data of Table IV show no systematic trend of properties with molding pressure, and indicate properties distinctly inferior to those of specimen 63J-2. A reduction in diametral restraint during the pressure-baking part of the molding cycle, produced by a reduction in molding pressure, did eventually eliminate macrocracks, but did not yield particularly good graphites.

2. Grinding Products: Seven hot-molded graphites were made from grinding products described in Table I. These are listed in Tables III and IV as specimen series 64. For ease in mixing, specimens 64F-1 and 64E-1 were made with 23S pitch binder, using solvent-blending and molding program A (described on page 10 of Report No. 12) and graphitizing in flowing helium at about 2800°C. Densities were low and other properties were not outstanding. All other specimens in this series were made with 30 MH pitch, and the same procedures were used for all but specimens 64H-3, for which molding pressure was reduced to 2000 psi, and 64H-2, for which it was 500 psi.

Specimens 64G-1 and 64H-1 have properties very similar to those of 63J-2, with even lower anisotropy and no apparent tendency to crack during molding. The fillers used to make them were produced by grinding the commercial Santa Maria LV lump coke in two stages of hammer milling at reasonably high rates. The reduced cracking tendency can probably be explained on the basis that the LV coke has been calcined at a higher temperature than was the filler used to make 63J-2, and so shrinks less during the pressure-baking part of the hot-molding cycle. This reduces the bulk density of the body in the baked condition. However, shrinkage during graphitizing is greater for the
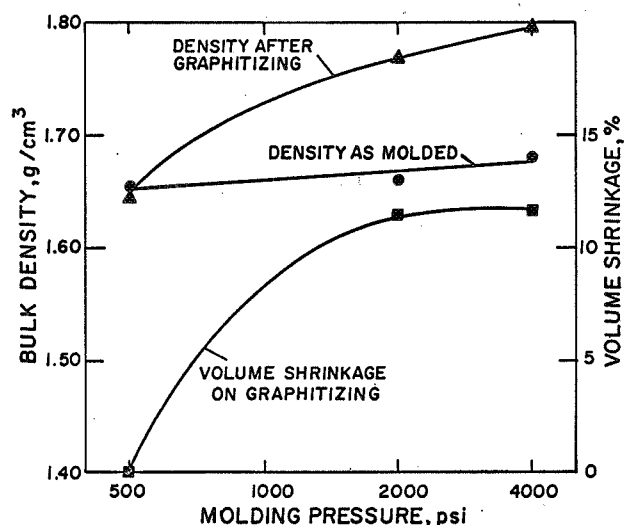
7

Fig. 4. Effect of molding pressure on bulk densities and volume shrinkage during graphitization, 64H graphites.

LV coke--which is not understood--and so densities after graphitization are essentially the same.

The effects of molding pressure on baked and graphitized densities and shrinkage during graphitization are summarized in Fig. 3 for the filler used in making specimens 63J-2, which had been vacuum-calcined at 900°C. Similar data are summarized in Fig. 4 for the "W + 2" filler of Table I, which had been calcined to a higher temperature. (These data represent specimens 64H-1, 64H-2, and 64H-3, which are listed in Table III.) In this case there are no maxima in the density and shrinkage curves, which rise continuously as molding pressure increases. An increase in calcination temperature of perhaps 200°C has significantly changed the shrinkage behavior of the coke as well as its grinding behavior. Obviously, both are important in affecting the properties of graphites made from Santa Maria fillers.

3. Resin-Bonded Graphites: Six hot-molded graphite specimens have been produced from Santa Maria graphite flour using a high-viscosity furfuryl alcohol resin binder, EMW-1600 (discussed in Report No. 12, pp 22-25). The filler used was CMF-13 Lot G-26 (also described in Report No. 12, page 4). Binder concentration in all cases

was 20 pph, including 0.5% maleic anhydride curing catalyst, except for specimen 63V-1 in which maleic anhydride concentration was 1.0%. Standard mixing techniques were used, with molding program "A", and graphitization was in flowing helium at about 2800°C. Densities, shrinkages, etc., for these graphites are summarized in Table V.

These are the first resin-bonded Santa Maria graphites so far produced using molding program "A" which have not exploded the die. (This program involves heating under 4000 psi pressure from 20 to 900°C at the relatively rapid constant rate of 50°C/hr.) This is probably due in part to use of an improved binder and in part to reduction in the catalyst concentration--which has usually been 4%.

During preparation of these specimens it was discovered that, although a mix prepared just prior to molding behaved normally, the same mix stored under refrigeration overnight in a sealed container would blow up the die. The reason for this behavior is not known.

4. Pitch-Bonded Graphites: Several additional hot-molded, pitch-bonded specimens, listed in Tables V and VI, have been made for a variety of purposes. In general these were solvent-blended, molded using program "A", and graphitized in flowing helium to 2800°C.

Specimens 63O-1 and 63P-1 were made to examine the behaviors of two experimental Santa Maria fillers acquired from the Y-12 Plant of Union Carbide Corporation. These are identified in Tables V and VII as CMF-13 Lots G-30 and G-31. (They were originally identified by Y-12 as Blends 3A and 3B. However their individual identities were lost during shipment.) Carbon black was added to both fillers, and the binder used was Barrett 30MH coal-tar pitch. Although the screen analyses of these two fillers were quite different from that of Lot G-26 (another Y-12 grind, further described in Report No. 12), their molding behaviors were quite similar to those of that earlier lot. The two graphites produced had moderate densities, with reasonable amounts of visible porosity and generally good structures. Microstructural examinations suggested that both fillers were deficient in particles in the size range about 10 to 30 μ diameter, which led to the

TABLE V

MANUFACTURING DATA, HOT-MOLDED GRAPHITES MADE FROM SANTA MARIA FILLERS

Speci- men No.	Filler Identi- fication	Binder Identi- fication	Conc., pph	Calculated Binder Optimum (a)	Binder Residue, % Baked	Graph.	Density, g/cm³ Packed Filler Baked	Graph.	Bulk Baked	Graph.	Dimensional Change, Baked to Graph., % Δl	Δd	Δv
63V-1	G-26	EMW-1600	20(b)	16.9	45.2	43.9	1.635	1.636	1.783	1.780	+0.5	-0.3	-0.0
63W-1	G-26	EMW-1600	20(c)	15.5	35.3	33.9	1.676	1.684	1.795	1.798	+0.3	-0.4	-0.5
63W-2	G-26	EMW-1600	20(c)	15.3	36.0	34.6	1.681	1.687	1.802	1.804	+0.4	-0.4	-0.4
63W-3	G-26	EMW-1600	20(c)	17.9	41.0	39.5	1.618	1.652	1.751	1.783	-1.3	-0.4	-2.0
63W-4	G-26	EMW-1600	20(c)	16.5	38.7	36.4	1.658	1.663	1.786	1.784	+0.3	-0.3	-0.3
63W-6	G-26	EMW-1600	20(c)	17.9	44.1	42.6	1.619	1.630	1.761	1.769	+0.3	-0.5	-0.7
63 O-1	G-30(d)	30MH	20	20.2	59.4	55.7	1.603	1.605	1.793	1.784	+0.6	-0.4	---
63P-1	G-31(d)	30MH	20	20.1	58.7	55.1	1.606	1.601	1.795	1.778	+0.7	-0.2	---
63U-1	G-32	23S	25	---	---	---	---	---	1.775	1.759	+0.6	0.0	---
64A-1	CP-15(e)	23S	20	---	---	---	---	---	1.637	1.691	-2.6	-2.8	---
64B-1(g)	CP-15(+T)(f)	23S	20	---	---	---	---	---	1.643	1.760	-3.9	-3.7	---
64C-1	CP-15(-30#)	23S	25	---	---	---	---	---	1.631	1.709	---	---	---
64C-3	CP-15(-30#)	23S	25	---	---	---	---	---	1.649	1.698	-3.1	-3.0	---
64D-1	CP-15	23S	25	---	---	---	---	---	1.644	1.688	-3.0	-3.0	---

(a) pph

(b) Including 1.0% maleic anhydride.

(c) Including 0.5% maleic anhydride.

(d) Thermax carbon black added in the proportion 15 parts Thermax to 85 parts filler.

(e) Thermax carbon black added in the proportion 30 parts Thermax to 70 parts filler.

(f) Thermax carbon black added in the proportion 35 parts Thermax to 65 parts filler.

(g) Cracked during molding.

the formation of many short microcracks between large filler particles and adjacent large volumes of binder residue.

Similarly, Specimen 63U-1 was made to investigate the molding behavior of CMF-13 Lot G-32 filler, another Y-12 experimental grind of Santa Maria coke (identified by Y-12 as Blend 2). In this case no carbon black was added to the filler and the binder was Barrett 23S coaltar pitch. Properties of the finished graphite are listed in Table VI, and are not exceptional.

CMF-13 filler Lot CP-15 was prepared from Santa Maria LV lump coke, Lot CL-6, using two stages of hammer milling--the "S + T" sequence. Its screen analysis is given in Table VII and is very much like that of Lot G-30, which was prepared by Y-12, also by hammer milling the calcined coke. Part of Lot CP-15 was given an additional "T" grind, and then identified as CP-15(+T). Another part was screened through 30 mesh, and the minus 30 mesh fraction was identified as CP-15(-30#).

The effect of Thermax carbon black additions on the packing behavior of Lot CP-15 was investigated using the stearic-acid technique, with the results plotted in Fig. 5. As has been observed with other Santa Maria fillers, two maxima occurred in the curve of packed filler density vs Thermax addition. It appears that about 30% Thermax should be the optimum addition to CP-15 filler.

TABLE VI

PROPERTIES OF HOT-MOLDED, PITCH-BONDED, SANTA MARIA GRAPHITES

Specimen No.	63U-1	64A-1	64B-1[d]	64C-1	64C-3	64D-1
Density, g/cm^3	1.759	1.691	1.760	1.709	1.698	1.688
Tensile Str., psi						
With-grain	1794[c]	---	1528[c]	2048	---	2018
Compr. Str., psi						
With-grain	---	5135	10,588	10,799	---	---
Across-grain	---	6094	10,489	11,354	---	---
Flexure Str., psi						
With-grain	2633	918	907	3508	3352	3195
Across-grain	2223	1081	2501	3331	2732	2578
Young's Mod., 10^6 psi						
With-grain	---	0.58	1.21	1.17	---	---
Across-grain	---	0.63	1.21	1.15	---	---
CTE, x 10^{-6}/°C [a]						
With-grain	---	5.58	5.73	5.66	---	---
Across-grain	---	5.63	6.00	5.76	---	---
Therm. Cond., W/cm-°C						
With-grain	0.87	0.47	0.49	0.96	---	0.89
Across-grain	0.81	0.47	0.45	0.85	---	0.81
Resistivity, $\mu\,\Omega$ cm						
With-grain	1649	3381	3255	1658	1616	1805
Across-grain	1771	3181	3131	1571	1557	1600
Anisotropies						
BAF[b]	1.050	~1.00	~1.00	1.027	1.024	~1.00
Compr. Str.	---	1.19	0.99	1.05	---	---
Flexure Str.	1.18	0.85	0.36	1.05	1.23	1.24
Young's Mod.	---	0.92	1.00	1.02	---	---
CTE	---	1.01	1.05	1.02	---	---
Therm. Cond.	1.07	1.00	1.09	1.13	---	1.10
Resistivity	1.07	0.94	0.96	0.95	0.96	0.89

(a) Coefficient of thermal expansion, average, 25-645°C.

(b) Bacon anisotropy factor, σ_{oz}/σ_{ox}.

(c) Broke in threads during tensile test.
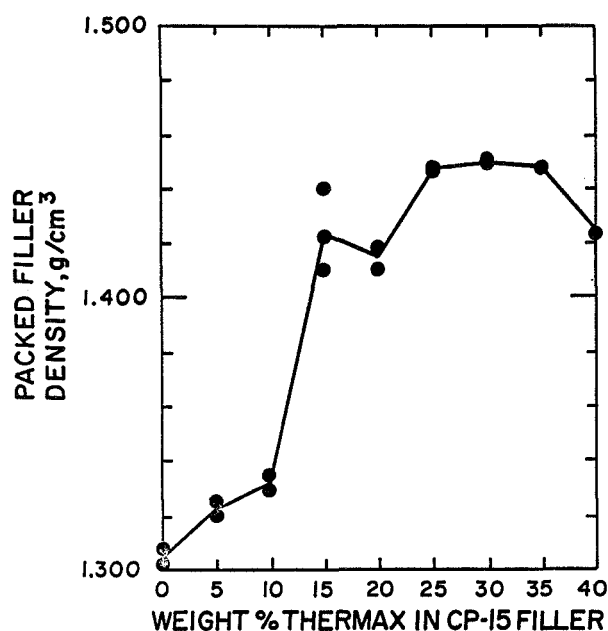
(d) Specimen cracked during molding.

Fig. 5. The effect of Thermax additions on the packed filler density of molded specimens made from hammer-milled Santa Maria coke, Lot CP-15.

Specimen 64D-1 was hot-molded and graphitized under normal conditions, using Barrett 23S coal-tar pitch and no Thermax addition to the CP-15 filler. Specimen 64A-1 was made similarly but with 30% Thermax added to the filler. Its density was essentially the same as that of 64D-1, and its other properties (listed in Table VI) were not as good. In this case the stearic-acid tests were misleading with regard to the effects of a Thermax addition, probably because they can not take into account the large effects of coke shrinkage during baking and graphitizing. The relatively poor properties of 64A-1 appear to result primarily from the presence of a network of microcracks within the binder residue and along interfaces between the binder and the filler particles. At least in part, these are probably also due to shrinkage of the coke, although a large deficiency of fine filler particles is believed to have been principally responsible for the cracking.

Specimen 64B-1, made from the finer CP-15 (+T) filler and with an even larger (35%) Thermax addition, cracked during molding. Its density was higher than that of 64A-1,

TABLE VII

SCREEN ANALYSES OF SANTA MARIA FILLERS

CMF-13 Lot No.	Weight Percent in Screen Fraction					
	+25	-25+45	-45+80	-80+170	-170+325	-325
G-26	0	Tr	3.8	19.6	21.2	55.4
G-30	0	Tr	10.6	59.6	19.4	10.4
G-31	Tr	Tr	12.6	48.6	21.2	17.6
CP-15	Tr	2.5	18.5	50.0	19.0	10.0

as were its strength and Young's modulus. Improved filler-particle packing as a result of the presence of higher proportions of fine and intermediate-size particles greatly reduced both the number and the maximum size of the microcracks.

Specimens 64C-1 and 64C-3 were made from the CP-15 filler after its plus 30 mesh fraction had been removed by screening. This improved the properties of graphites made from it only slightly. It did, however, reduce the number of microcracks. Where they were present, the microcracks usually occurred along the edges of the larger filler particles.

III. HIGHLY ORIENTED POLYCRYSTALLINE GRAPHITES

A. Previous Work

CMF-13 investigations of the manufacture and properties of highly oriented polycrystalline graphites have previously been discussed in Reports No. 7, 8, 10, 11, and 12 in this series.

B. Natural Graphite Fillers (R. J. Imprescia)

Most of the experimental highly oriented graphites so far manufactured by CMF-13 have been made from the same very fine natural-graphite filler, Southwestern Graphite Company's Grade 1651 (CMF-13 Lot No. G (Na)-21), which is 100% minus 325 mesh. Three other, somewhat coarser grinds of natural graphite flakes have recently been obtained from the same company and are now being evaluated for use as fillers. These fillers and their screen analyses are listed in Table VIII.

11

TABLE VIII

SCREEN ANALYSES OF NATURAL GRAPHITE FILLERS

CMF-13 Lot No.	Mfr. Grade	Weight Percent in Screen Fraction				
		+45	-45+80	-80+170	-170+325	-325
G(Na)-21	1651	0	0	0	0	100.0
G(Na)-22	1652	0	0	0	Tr.	99.9+
---	1645	0	Tr.	0.5	4.5	95.5
---	1641	0	Tr.	3.0	29.0	68.0

TABLE IX

DENSITIES, BINDER RESIDUES, AND SHRINKAGES OF HOT-MOLDED GRAPHITES

MADE FROM NATURAL GRAPHITE FILLERS

Speci-men No.	Filler		Calculated Binder Optimum (a)	Binder Residue, %		Density, g/cm³				Dim. Change,%, Baked to Graph.	
	Mfr. Grade	Percent -325#		Baked	Graph.	Packed Filler Baked	Packed Filler Graph.	Bulk Baked	Bulk Graph.	$\Delta \ell$	Δd
59S-1	1651	100.0	16.2	48.3	31.2	1.769	1.736	1.940	1.845	+1.6	+0.1
59T-1	1652	99.9	13.7	40.0	16.8	1.831	1.798	1.977	1.857	+1.5	+0.7
59R-1	1645	95.5	---	---	---	---	---	2.009	1.881	+2.0	+0.1
59R-3	1645	95.5	---	---	---	---	---	2.011	1.882	+2.2	+0.2
59Q-1	1641	68.0	11.0	35.9	12.1	1.908	1.852	2.045	1.897	+2.3	+0.3
59V-1	1651 [b]	100.0	---	---	---	---	---	1.699	1.467	+8.1	+1.5
59U-1	1651 [c]	100.0	---	---	---	---	---	1.719	1.492	+7.1	+1.7
59P-1	1651 [d]	100.0	---	---	---	---	---	1.667	1.439	+7.4	+1.9
59W-1	1651 [e]	100.0	---	---	---	---	---	1.688	1.455	+6.6	+2.3

(a) pph. Binder used was 20 pph of 23S coal-tar pitch.

(b) Plus 5 pph Kynol. Contained large delamination cracks.

(c) Plus 10 pph Kynol. Contained a few delamination cracks.

(d) Plus 15 pph Kynol. Some delaminations.

(e) Plus 20 pph Kynol.

Pitch-bonded, molded specimens have been made from each of these fillers using standard CMF-13 procedures. Barrett Grade 23S coal-tar pitch was used as binder, in the proportion 20 parts pitch to 100 parts filler, by weight. Solvent blending, with tetrahydrofuran, was followed by hot chopping, hot molding according to program "A", and graphitizing in flowing helium at about 2800°C. The specimens produced and their densities and shrinkages are listed in Table IX. Binder concentrations used were in all cases higher than were actually required. With mixes 59R-1 and 59R-3 an unusual amount of sticking of punches to specimens occurred, making it impossible to make the measurements required to calculate binder residues and packed filler densities.

Properties of these graphites are summarized in Table X. As the natural-graphite filler becomes coarser the particles pack more densely, binder requirement decreases, and bulk density increases. There is no clear

trend of degree of preferred orientation or anisotropy of properties. Flexure strength decreased significantly with coarsening of the filler. In all samples the principal defects were lenticular pores, formed either by cleavage of filler flakes or by shrinkage of binder residues adjacent to the flakes.

C. Kynol Fiber Additions (R. J. Imprescia, J. M. Dickinson)

As was discussed in Report No. 12 in this series, Kynol fibers appeared to fuse when they were heated under pressure. This suggested that they might be useful not only as a filler reenforcement but perhaps also as a binder. To investigate this possibility, four hot-molding runs, listed in Tables IX and X as 59V-1, 59U-1, 59P-1 and 59W-1, were made in which the conventional binder was replaced with Kynol. The filler was Grade 1651 natural graphite flour, to which 5 to 20 pph of Kynol were added. Standard dry, twin-shell blending was used, followed by hot-molding (Cycle A) and graphitization in flowing helium to 2800°C. In a fifth run, not listed in the tables, Lot G-26 Santa Maria graphite flour was used as filler with 20 pph of Kynol. In this case no apparent bonding occurred during molding, and the charge was ejected from the die as an unconsolidated mass of loose fibers and powder.

Three of the four natural-graphite specimens showed obvious delamination cracking when ejected from the die. The fourth (59W-1) appeared to be sound. However, subsequent microscopic examination revealed internal delamination cracks in all four specimens, approximately normal to the molding axis, with the extent of delamination increasing with fiber content. Associated with each of the fibers was a parallel void, apparently developed by shrinkage of the fiber and nearly as large as the fiber residue. The fiber residues were oval in section and showed optical anisotropy indicating graphitization, with the average orientation of basal planes normal to the molding axis.

All four of these specimens showed a high degree of preferred orientation and anisotropy. However, all expanded greatly on graphitizing, had low densities, and were very weak. Electrical resistivities were high, especially in the across-grain direction, indicating the presence of many internal discontinuities.

At least used alone, Kynol does not appear promising as a binder material.

An attempt was made to extrude a resin-bonded graphite in which 16% of the graphite flour filler was replaced by Kynol fibers. At very low extrusion rates the green rod emerged from the die normally but after a few seconds began to swell. The diameter increase exceeded 25%, and many cracks were formed. In subsequent molding experiments with the same mix it was found that the swelling was less severe if the material was held under pressure in the die for several minutes. Accordingly, the extruded rods were chopped and the chopped mix pressed at room temperature in a 1.5 in. dia steel die, with the molding pressure of 15,000 psi maintained for either 20 or 40 min. A reduction in spring-back resulted, although in all cases final bulk densities were low. The highest density produced was 1.405 g/cm^3, in a specimen which had been held under pressure for 40 min.

D. Hot-Molded Cones (R. J. Imprescia)

Small, hot-molded hemispheres have previously been produced from pitch-bonded flake natural graphite. As was described in Report No. 9, these were not of high density, and contained pronounced density gradients. However, under certain conditions, sound hemispheres were produced having highly preferred filler-particle orientations in desirable relations to the surfaces of the hemisphere. The technique has therefore been extended to the production of conical shapes.

Specimen 60B-1 was a flat-ended, hollow, 60° cone about 3 in. outside diameter at the large end and 2 in. high, with a wall about 7/16 in. thick. It was made from a solvent-blended mix containing 85 parts G(Na)-21 natural flake graphite, 15 parts Thermax carbon black, and 22 pph Barrett 30MH coal-tar pitch. Molding was by the standard "A" cycle except that pressure was reduced to 2000 psi, and graphitization was in flowing helium at 2800°C. After a feathered edge at its large end was removed, the cone was sound and free of cracks. Overall density was 1.71 g/cm^3, which is low for this mix, presumably because of the relatively low molding pressure

TABLE X

PROPERTIES OF HOT-MOLDED GRAPHITES MADE FROM NATURAL GRAPHITE FILLERS

Specimen No.	59S-1	59T-1	59R-1,3	59Q-1	59V-1	59U-1	59P-1	59W-1
Density, g/cm^3	1.845	1.857	1.881	1.897	1.467	1.492	1.439	1.455
Flexure Str., psi								
With-Grain	3447	2738	2360	1921	618	691	726	787
CTE, x 10^{-6}/°C [a]								
With-Grain	1.69	1.79	1.48	1.81	---	---	---	---
Across-Grain	10.32	9.77	9.19	8.90	---	---	---	---
Resistivity, $\mu\,\Omega$ cm								
With-Grain	857	740	759	727	1514	1429	1205	1156
Across-Grain	3836	3322	2994	3189	13,599	11,830	16,840	17,744
Anisotropies								
BAF [b]	2.73	3.14	2.40	2.65	4.29	4.21	4.28	4.10
CTE	6.11	5.46	6.21	4.92	---	---	---	---
Resistivity	4.48	4.49	3.94	4.39	8.99	8.28	13.98	15.35

(a) Coefficient of thermal expansion, average, 25-645°C.

(b) Bacon anisotropy factor, σ_{oz}/σ_{ox} .

used. Dimensional changes during graphitization were essentially zero, indicating that good dimensional control is possible. At the flattened end of the cone a high degree of preferred orientation was produced, with the crystallites approximately parallel to the flat inner and outer surfaces. In this region, bulk density was distinctly higher near the inner surface (1.73 g/cm^3) than near the outer surface (1.60 g/cm^3). Along the skirt of the cone the degree of preferred orientation was about as high as at the end, but here the filler flakes were inclined at about 12° to the external surface, making a larger angle with the cone axis than did that surface. (Thus, along this surface, the filler flakes overlapped like shingles on a conical roof--which appears to be a desirable arrangement for resisting particle detachment in an ablative environment.) Here bulk density ranged from 1.69 to 1.72 g/cm^3.

Subsequent attempts to produce a round-nosed cone with a 40° included angle have not so far been successful, due usually either to cracking or to sticking to the punch. Various fillers, molding procedures, and die designs are being tried in an attempt to overcome these difficulties.

IV. CARBON BLACKS

A. General (R. D. Reiswig)

Carbon black is a very common addition to the raw mixes from which commercial carbons and graphites are made. It is usually assumed that its principal functions are to improve manufacturing behavior and increase bulk density by lubricating the motion of filler particles past each other and by filling small voids between them. CMF-13 observations indicate that the carbon black particles are normally suspended in the binder, replacing part of it, reducing its shrinkage as it is cured and pyrolyzed, and so reducing the incidence of microcracks within the binder residue and at filler-binder interfaces.

CMF-13 has so far usually used Thermax carbon black in the manufacture of experimental graphites. This is a relatively coarse black (mean particle diameter 0.33 μ) manufactured by Thermatomic Carbon Co. and described in detail in Report No. LA-3981. A typical mix

TABLE XI

CHARACTERISTICS OF CARBON BLACKS

CMF-13 Lot No.	Manufacturer	Grade	Mean Particle Diameter, μ		BET Surface Area, M^2/g
			Mfr. Data	CMF-13 Data	
TP-33	Thermatomic Carbon Co.	P33	0.15	0.22	12.4
TP-4	Thermatomic Carbon Co.	Thermax	0.35	0.33	8.9
T-9	Cabot Corporation	MT	0.47	<0.47	6.
T-10	Cabot Corporation	MTNS	0.47	<0.47	6.

formulation for production of an extruded, resin-bonded graphite is, by weight, 85 parts graphite flour, 15 parts Thermax, and 27 parts binder. If it is assumed that all of the Thermax particles are spherical, 0.33μ dia, and uniformly distributed throughout the binder, the calculated distance of closest approach (surface-to-surface) of these particles is approximately equal to their average diameter. There are at least two reasons why substitution for the Thermax of a still coarser black, in the same weight proportion, might be advantageous: (1) The degree to which the residue of a furfuryl alcohol resin binder (and perhaps of other binders) graphitizes is strongly influenced by the presence within it of solid particles. This is believed to be a mechanical effect produced by shrinkage of the resin around an essentially incompressible particle, stretching the polymer, aligning its molecular components, and predisposing it to form a layered graphite structure during subsequent heat treatment. If this is correct, the use of a coarser black might increase stretching of the polymer, improve its molecular alignment, and finally yield a better-graphitized binder residue. This should, for example, increase electrical and thermal conductivity of the finished graphite. (2) If the same weight proportion of a coarser black is used in the mix, the mean free path for any process occurring between particles increases in proportion to the diameter of the carbon black particles. The results of this increase might include easier escape of gases during curing and baking, as well as further improvement of transport properties.

B. Commercial Carbon Blacks (L. S. Levinson, H. D. Lewis)

The commercial carbon black having the largest advertised mean particle size so far encountered is Sterling MT black, produced by the Cabot Corporation. Its quoted average particle diameter is only about 1.35 times that of Thermax, but attempts to find a source of still coarser blacks have so far been unsuccessful. Accordingly, samples of MT and MTNS carbon black have been obtained from the Cabot Corporation. The latter is a "non-staining" MT carbon black which has been heat-treated to about 1000°F.

Small samples of the MT and MTNS blacks (CMF-13 Lots T9 and T10, respectively) were ultrasonically dispersed in a 0.25% Aroplaz-xylene solution for electron-microscope examination. In both cases the individual particles were essentially spherical, and the maximum particle diameter found was about 0.5μ. Insufficient measurements were made to determine a mean particle diameter, but in both samples this appeared to be significantly less than the 0.47μ stated in the Cabot literature, and significantly greater than the 0.33μ previously measured for Thermax carbon black. Surface areas, measured by BET nitrogen-adsorption, were significantly less than that of Thermax, also indicating a somewhat larger mean particle diameter. These measurements are summarized in Table XI, which also lists corresponding information on Thermax carbon black and Thermatomic Carbon Co. Grade P33 carbon black (which was discussed in Report No. 5 in this series). Both Thermax and Grade P33 also consist of essentially spherical particles.

TABLE XII

MANUFACTURING DATA, EXTRUDED GRAPHITES MADE WITH A VARIETY OF CARBON BLACKS

Graphite Lot No.	Mix Composition						Extrusion Conditions			
	Filler		Carbon Black		Binder		Pressure, psi	Velocity, in./min.	Temperature, °C	
	Lot No.	pph	Lot No.	pph	Type	pph			Mix	Chamber
ACO3	G-18	85	TP-33	15	Varcum [a]	27	5150	167	44	43
ACO7	G-18	85	TP-33	15	Varcum [a]	27	6950	171	45	50
ACO4	G-18	85	TP-4	15	Varcum [a]	27	5400	156	44	45
ACO2	G-18	85	T-9	15	Varcum [a]	27	---[b]	---	---	---
ACO5	G-18	85	T-9	15	Varcum [a]	27	5500	176	44	44
ACO1	G-18	85	T-10	15	Varcum [a]	27	6300	171	43	45
ACO6	G-18	85	T-10	15	Varcum [a]	27	---[b]	---	47	45
ACO8	G-18	85	T-10	15	Varcum [a]	27	5400	164	43	55

[a] Varcum 8251.

[b] Severe pressure oscillations; extrusion discarded.

C. Extruded Graphites (J. M. Dickinson)

The ACO series of resin-bonded, extruded graphites was made to investigate the effects of varying the particle size of the carbon black addition, using the four commercial blacks listed in Table XI. In all cases the principal filler material was 85 parts of Great Lakes Grade 1008-S graphite flour (CMF-13 Lot No. G-18) which was mixed with 15 parts of carbon black and 27 parts of Varcum 8251 furfuryl alcohol resin binder containing 4% maleic anhydride curing catalyst. Compositions and curing conditions are listed in Table XII. Extrusion Lots ACO2 and ACO6 were discarded in the green state due to defects caused by pressure pulsations during extrusion. All other lots were cured, baked, and graphitized to 2800°C together. Properties so far measured on the finished graphites are listed in Table XIII.

Use of the slightly coarser Cabot carbon blacks appears to have produced small increases in bulk density and carbon residue, with no significant effect on electrical resistivity. However, it is possible that extrusion difficulties may have contributed to the rather low density and carbon residue of Lot ACO4, made with Thermax carbon black. Some of these extrusions will be repeated, and the search for a still coarser carbon black will be

continued.

V. BINDERS

A. Characterization of EMW 1600 (E. M. Wewerka, H. D. Lewis)

EMW 1600 is a relatively large lot of acid-polymerized furfuryl alcohol resin produced in CMF-13 by polymerizing directly to a viscosity of about 1600 cp. It has been used as binder in the manufacture of several series of both extruded and molded experimental graphites, and has shown some advantages over the lower-viscosity commercial resin--Varcum 8251--which has normally been used. A statistical comparison of the molecular-size distributions of the two resins has been made and is summarized in Table XIV. In agreement with previous qualitative comparisons, these data show that EMW 1600 has a larger "mean molecular size" than does Varcum 8251, and-- based on the tabulated values of "variance" and "coefficient of variation"--also has a narrower molecular size distribution. Both of these properties are believed to be desirable when the resin is used as a binder in graphite manufacture.

TABLE XIII

PROPERTIES OF EXTRUDED GRAPHITES MADE WITH VARIOUS CARBON BLACKS

Graphite Lot No.	Carbon Black Identification	Bulk Density, g/cm^3	Carbon Residue, %	Electrical Resistivity, $\mu\,\Omega\,cm$	Young's Modulus, 10^6 psi
ACO3	P33 (Fine)	1.855	44.2	1172	$2.33 \pm .03$
ACO7	P33 (Fine)	1.863	45.6	1159	$2.39 \pm .04$
ACO4	Thermax (Medium)	1.855	44.5	1152	$2.35 \pm .02$
ACO5	MT (Coarse)	1.883	46.6	1182	$2.29 \pm .02$
ACO1	MTNS (Coarse)	1.876	46.2	1135	$2.48 \pm .04$
ACO8	MTNS (Coarse)	1.881	46.4	1133	$2.49 \pm .03$

TABLE XIV

COMPARISON OF TWO FURFURYL ALCOHOL BINDER RESINS

Identification	Viscosity, cp	Mean Size, $\bar{x}$	Variance, s_x^2	Skewness, g_x	Coefficient of Variation, CV_x
Varcum 8251	250	2.41	1.22	0.098	0.456
EMW 1600	1600	2.54	0.67	44.2	0.323

B. Identification of Resin Components (E. M. Wewerka)

As the individual components of furfuryl alcohol resins have been isolated and identified, a name (or names) has been assigned to each which has been based more on ease of oral communication than on convention. Consequently some of the names which have appeared in CMF-13 reports, although not incorrect, have been common only within the group and may have been confusing to other readers of these reports. To avoid further confusion, more conventional names have been assigned to some of these molecular species. The structural formulae and conventional names of the resin components of interest in this regard are listed in Table XV. CMF-13 will attempt to adhere carefully to these names (or abbreviations of them) in future reports and communications.
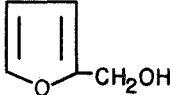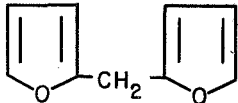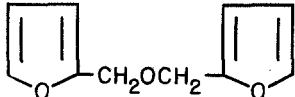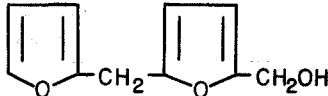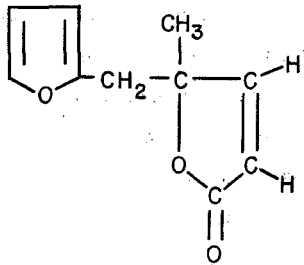
The principal technique used by CMF-13 to determine the presence and amount of each of these components is gel-permeation chromatography ("GPC"). The column system currently used in the GPC apparatus consists of five columns in series, each 4 ft long, with maximum pore diameters of 3000, 500, 250, 250, and 60 Å respectively. A continuous record is made of the refractive index of the solution leaving the final column, and a pip is made on the recorder chart after each 5 ml of solution has passed through the refractometer. The number of "counts"--i.e., of pips--since the sample was injected into the first column is an indication of the time required for the corresponding fraction of the solution to pass through the system, and so of the molecular size of the species present in that fraction.

Samples of each of the low-molecular-weight species found in furfuryl alcohol resins, separated by gas chromatography, were injected into the GPC unit and their elution positions were recorded in terms of the number of counts between injection and appearance on the chart. These positions are listed in Table XV for each of these resin components.

Most of the furfuryl alcohol resin components isolated by gas chromatography can originate as primary reaction products during polymerization of furfuryl alcohol. However, difurylmethane and its next higher homolog are

17

TABLE XV

IDENTIFICATION OF RESIN COMPONENTS

Structure	Name	Elution Position, Counts
	Furfuryl alcohol (monomer)	35.8
	Difurylmethane	36.0
	Difurfuryl ether	35.0
	5-Furfuryl-furfuryl alcohol (dimer)	34.0
	2,5-Difurfuryl Furan	34.1
	4-Furfuryl, 4-methyl, 2-en, γ -butyrolactone	34.4

believed to be secondary products resulting from cleavage of other, primary reaction products. Therefore it also seemed possible that some--or all--of the difurylmethane isolated by gas chromatography was produced by partial decomposition of difurfuryl ether or dimer during the chromatographic separation, and was not present as difurylmethane in the original resin. To test this, difurfuryl ether and dimer were collected from the gas chromatograph, and each was reinjected as a pure sample. No difurylmethane was detected, nor was an appreciable amount of any other decomposition product of either material. From this it appears that isolated furfuryl alcohol resin components are relatively stable, at least over short periods of time, when subjected to temperatures well above those at which thermal polymerization and curing of the bulk resin are usually observed. Further, samples of individual components separated from the resin by gas chromatography are evidently representative of the concentrations of those components in the original resin.

TABLE XVI

DISTRIBUTIONS OF LOW-MOLECULAR WEIGHT COMPONENTS IN FURFURYL ALCOHOL RESINS

| Component | Acid-Polymerized Resin | | γ-Alumina-Polymerized Resin | | | |
| | | | In-situ Polymerization | | Column-Reflux Polymerization | |
	% of Low M. W. Fraction	% of Total Resin	% of Low M. W. Fraction	% of Total Resin	% of Low M. W. Fraction	% of Total Resin
Furfuryl Alcohol	59	21	22	9	20	7
Difurylmethane	9	3	11	4	6	2
Difurfuryl Ether	10	4	41	16	38	14
Dimer	18	7	--	--	--	--
γ-Butyrolactone	--	--	20	8	26	9
2,5-Difurfuryl Furan	4	1	6	3	6	2
Water	Tr	Tr	Tr	Tr	4	1
Total Accounted For:	100%	36%	100%	40%	100%	35%

C. Components of Acid-and Alumina-polymerized Resins

(E. M. Wewerka)

All low-molecular-weight components separated by gas chromatography from furfuryl alcohol resins polymerized with acid catalysts and with γ-alumina have been analyzed by nuclear magnetic resonance methods to confirm their structures and investigate their purities. The NMR spectrum of each component correlated nicely with the structure that had previously been assigned to it. As indicated by the absence of extraneous NMR bands, each of the separated materials was relatively pure except for the γ-butyrolactone, which evidently contained a small proportion of some foreign material. The nature and concentration of this impurity have not yet been determined.

Gas-chromatography analyses have been repeated on an acid-polymerized furfuryl alcohol resin and two γ-alumina-polymerized furfuryl alcohol resins, each with a viscosity of about 300 cp. The concentration of each component in each resin as determined gas chromatography is listed in Table XVI. The components listed account for essentially all of the low-molecular-weight material initially separated from the resins by distillation, and for 35 to 40% of the weights of the original resins.

As has previously been reported, the alumina-polymerized resins differ from the acid-polymerized ones principally in containing the γ-butyrolactone component,

much greater proportions of difurfuryl ether, and no detectable furfuryl alcohol dimer. The smaller concentrations of furfuryl alcohol in the alumina-polymerized resins probably reflect primarily the facility with which difurfuryl ether and γ-butyrolactone form in that system. However, they are probably also affected by loss of furfuryl alcohol at the exit of the reflux condenser when high temperature is attained during resin polymerization.

In a furfuryl alcohol resin, only those components containing hydroxymethyl groups (such as furfuryl alcohol and the furfuryl alcohol dimer) are capable of increasing the sizes of other molecules in the system by combining with them. When a molecule containing a hydroxymethyl group combines with another which does not, then chain propagation ceases. Thus, reaction of the furfuryl alcohol monomer with difurylmethane yields 2,5-difurfuryl furan, which contains no hydroxymethyl group and cannot cause further polymerization. About 80% of the components isolated from the low-molecular-weight fractions of γ-alumina-polymerized resins were of the terminating or non-propagating type, and the chemistry of the higher-molecular-weight fractions of these resins is probably similar to this. In alumina-polymerized resins, then, not enough molecules with propagation capabilities are present to have much effect on the larger number of non-propagating molecules and, when such a resin is used as

TABLE XVII

MANUFACTURING DATA, EXTRUDED PITCH-BONDED GRAPHITES

Graphite Lot No.	Mix Composition			Extrusion Conditions					
	Filler		Thermax, pph	23S Pitch, pph	Pressure, psi	Velocity, in./min	Temperature			Vacuum, Torr
	Lot No.	pph					Mix	Chamber	Die	
ACM1	G-18	85	15	35	18,000	30	80	80	85	450
ACM2[a]	G-18	85	15	30[b]	23,100	30	90	90	100	300
ACM3a[a]	G-26	85	15	30[c]	---	---	---	---	---	---
ACM3	G-26	85	15	31.73	13,500	164	102	100	100	700
ACM4	G-18	85	15	34	13,275	150	105	120	105	300
ACM5[a]	G-18	100	0	35[b]	---	---	105	125	100	350
ACM6	G-18	85	15	34[d]	9,000	171	110	130	105	300
ACM7[a]	G-18	100	0	38[b]	12,900	111	100	130	80	400

(a) Green extrusions contained serious defects and were discarded.

(b) Insufficient binder; extrusion cracked.

(c) Stalled food-chopper; more binder or lubricant required.

(d) Extrusion oil added, 2.7% of binder weight.

a binder, most of the latter molecules will not polymerize further during the curing cycle. In acid-polymerized resins, however, about 75% of the molecules isolated from the low-molecular-weight fraction were either furfuryl alcohol or furfuryl alcohol dimer, both of which are capable of increasing the sizes of other molecules. It is therefore clear why the acid-polymerized resins have in general given higher carbon residues when used as binders than have alumina-polymerized resins of similar viscosity. Although the monomer is not a particularly desirable component of a binder resin, at least some of it polymerizes during curing and eventually contributes to a larger extent to the carbon residue. It is at least less undesirable than the non-propagating species found in high concentration in alumina-polymerized resins, much of which vaporizes during the heat treatment instead of polymerizing further.

D. Polyphenylene Resins (E. M. Wewerka)

A survey of polyphenylene resins has been undertaken in the hope that one or more of them may be developed which will be useful as a binder material for graphite manufacture. Three polyphenylenes have so far been synthesized and examined.

Polyphenylene No. 1 is a linear p-polyphenylene, whose structure is similar to a series of benzene rings linked end to end. It is a brown, infusible, insoluble solid, with a porous, flocculent microstructure. It shows no evidence of fusion during heating to 1000°C, although some reduction in degree of crystallinity resulted from this heating. Thermogravimetric analysis under nitrogen yields about 50% carbon upon heating to 1000°C. Differential thermal analysis in air shows a large oxidation exotherm near 600°C, and continued oxidation results in complete loss of the material below 1000°C. Infrared analysis of the polymer shows bands associated principally with para type aromatic substitution.

Polyphenylene No. 2 is a 1:1 copolymer of biphenyl and m-terphenyl. In differential thermal analysis under nitrogen, no fusion point was detected. However, the resin particles appeared to have fused together after the DTA treatment. Infrared spectra contained bands associated with ortho, meta, and para substitutions.

Polyphenylene No. 3 was prepared by polymerizing

TABLE XVIII

PROPERTIES OF EXTRUDED PITCH-BONDED GRAPHITES

Graphite Specimen No.	Carbonization Rate, °C/hr	Bulk Density, g/cm^3	Binder Carbon Residue, %	Electrical Resistivity, $\mu\Omega$ cm	Young's Modulus, 10^6 psi
ACM1-1[a]	10°/hr to 900°C	Low	---	---	---
ACM1-2[a]	5°/hr to 900°C	Low	---	---	---
ACM1-3[b]	2.5°/hr to 200°C	Low	---	---	---
ACM3-2,4 6, 8, 9	10°/hr to 900°C	1.540	38.6	3165	0.67
ACM3-1, 3 5,7,10,11	2.5°/hr to 900°C	1.600	49.1	2590	0.84
ACM4-2, 9	5°/hr to 900°C	1.579	50.4	2106	---
ACM4-3, 7	2.5°/hr to 900°C	1.574	47.1	2245	---
ACM4-4, 8	1.25°/hr to 900°C	1.583	48.1	2180	---
ACM4-5	5°/hr to 900°C [c]	1.596	49.9	2163	---
ACM6-2, 9	5°/hr to 900°C	1.527	47.3	2493	---
ACM6-3, 7	2.5°/hr to 900°C	1.526	45.7	2334	---
ACM6-4, 8	1.25°/hr to 900°C	1.528	44.8	2335	---

(a) Badly cracked.

(b) Badly cracked, but better than specimens ACM1-1 and -2.

(c) Carbonized under pressure.

biphenyl, with the expectation that the properties of the polymer would be similar to those of ρ -polyphenylene. However, reaction conditions were difficult to control and there were large losses of biphenyl by sublimation. The reactants thickened rapidly to the point where they could not be stirred. The polymerization product did not look like ρ -polyphene and still contained large amounts of biphenyl. Polymerization conditions are being modified in an attempt to produce the desired resin.

E. Pitch-Bonded Extruded Graphites (J. M. Dickinson)

Because of the low capacity (40 tons) of the CMF-13 extrusion press, it has generally been possible to extrude pitch-bonded mixes only if a large excess of pitch was used. The ACM series of graphites was manufac-tured primarily to explore the possibility of extruding mixes in which a pitch having a very low softening point was used in normal concentrations. The pitch investigated was Barrett 23S, whose softening point is 54°C. In most cases the filler was Great Lakes 1008-S graphite flour, CMF-13 Lot G-18. However, graphites ACM3 and ACM3a (Table XVII) were made from a Santa Maria graphite flour, CMF-13 Lot No. G-26. In all but two cases 15 pph of Thermax carbon black was added. The binder pitch was diluted with tetrahydrofuran and mixed with the filler and carbon black in a twin-shell blender. The mix was then chopped in a food-chopper, which served not only to improve mixing but also to remove the solvent and warm the mix to the desired extrusion temperature, 100°C. It was then extruded, and was usually rechopped and ex-

truded a second and a third time.

Extrusion conditions for these graphites are summarized in Table XVII, and their properties in Table XVIII. Binder requirements were high, and large cracks appeared if the mix was too dry. Green diameters were not measured on all of the extrusions, but in general they were considerably larger than those of resin-bonded graphites extruded through the same die (e.g., 0.510-in. green dia from a 0.500-in. dia die). Extrusion pressures were higher than is usual for graphites bonded with furfuryl alcohol resins, but were well within the capabilities of the press.

Graphites ACM1 and ACM3 were baked to 900°C using heating rates of 2.5 to 10°/hr. The lower rates yielded better graphites, but did not completely eliminate cracks. Therefore the still lower rate of 1.25°C/hr was also used for graphites ACM4 and ACM6. Rod 5 of Lot ACM4 was baked under pressure at the relatively high rate of 5°C/hr. This sample was inserted into a 9/16-in. dia axial hole in a graphite rod 2.5 in. dia and 10 in. long, and the hole was sealed at each end with a threaded plug. Sample and holder were then heated in static helium in a sealed tube furnace equipped with a pressure-relief valve set at 30 psi. The pressure inside of the graphite holder is not known, and may have been higher than 30 psi.

All specimens except ACM4-4 (heated at 1.25°C/hr) and ACM4-5 (heated under pressure) showed some damage. Damage was reduced by slower heating--which, unfortunately, extrapolates to baking cycles of weeks or months. In spite of reasonably high binder-carbon yields, densities were low, which can be attributed in part to the low green densities resulting from expansion of the extruded rod as it left the die. One bright spot, however, was the behavior of the pressure-baked specimen, Rod ACM4-5. This had the highest density of any of the rods, was crack-free, and had relatively high carbon residue.

Further work on pitch-bonded extruded graphites will be directed principally toward understanding low-pressure carbonization and its usefulness in manufacturing graphite.

VI. POROSITY EFFECTS

A. Effects of Porosity on Elastic Properties (P. E. Armstrong)

The effects of porosity on Young's modulus, the shear modulus, and Poisson's ratio of commercial Poco graphites were discussed in Reports No. 11 and 12 of this series. Large changes in all three properties were reported as a result of heat-treatment of the samples to about 2900°C, in spite of the fact that some of the grades tested were purchased in the "-9Q" condition, indicating that they had already been heat-treated to 2900°C by the manufacturer.

These measurements were made on specimens 0.25-in. dia and 1.125-in. long. They have since been repeated on additional Poco graphite specimens 0.5-in. dia and 4-in. long, whose room-temperature properties were determined in the as-received condition and after heat-treatment in flowing helium to 2900°C. Results were within about 5% of those from the previous measurements.

Examination of these data and of similar data for powder-metallurgically prepared metallic tungsten showed that the elastic modulus vs void fraction relationship was similar for the two materials. With the assistance of LASL C-Division, fits of the modulus data were made to the theory of Mackenzie concerning this relation. It was found that neither material fit the Mackenzie theory exactly unless a term representing a distribution of pore sizes and another term representing a contribution of the order of the cube of the porosity were introduced. The validity of such a treatment is under study.

B. Effects of Porosity on Thermal Conductivity (P. Wagner)

Specimens machined from the 0.5-in. dia samples of Poco graphites discussed above are being used for measurements of electrical resistivity and thermal diffusivity at room temperature before and after heat-treatment to 2900°C. Preliminary results on 15 specimens, all of which had been heat treated to 2900°C, indicate that thermal conductivity is an essentially linear function of the

reciprocal of the fractional porosity of the graphite. This is consistent with the concept discussed below that the principal resistance to heat flow in graphite is provided by phonon scattering mechanisms.

VII. PHONON SCATTERING IN GRAPHITE
(P. Wagner)

Attempts have been made by several investigators to analyze the mechanism of thermal conduction in graphite, with varying degrees of success. One aspect of this problem is considered here: the prediction and observation of the effects on thermal conductivity of controlled alterations in the structures of certain graphites. These effects are interpreted in terms of a standard, simplified formulation which describes phonon-scattering processes. Since predictions from this formulation are consistent with experimental observations of the effects of defects, impurities, and low temperatures, this approach is believed to merit further attention.

A. Theory

Heat is conducted in graphite by two major mechanisms: electronic motion, and excitation of the acoustic vibrational modes in the graphite lattice. To a very good approximation, these modes are independent, and the total thermal conductivity (λ) may be written as the sum of the electronic (λ_ϵ) and lattice (λ_L) components:

$$\lambda = \lambda_\epsilon + \lambda_L \tag{1}$$

Efforts to evaluate these components individually in graphite have so far been unsuccessful, and in the present work this aspect of the problem has not been treated. Instead λ_L is considered without reference to λ_ϵ. In this instance the generality of the results appears not to have been affected by the omission. This is because, while total thermal conductivity is given by (1), at room temperature (300°K) $\lambda_L > \lambda_\epsilon$ and the expression

$$\lambda = \lambda_L , \tag{2}$$

while not exact, is a very reasonable approximation.

The lattice contribution to thermal conductivity is limited by the various primary phonon-scattering processes which can occur at crystallite boundaries, at defect or impurity sites of almost any kind, or as a result of phonon-phonon interactions (Umklapp processes). In general, where a single mean free path (ℓ) can be defined for each class of scatterer, the resultant mean free path is properly determined from the sum of all of the individual scattering probabilities, according to the equation:

$$\frac{1}{\ell} = \frac{1}{\ell_B} + \frac{1}{\ell_U} + \frac{1}{\ell_D} \tag{3}$$

where ℓ_B = mean distance between crystallite boundaries;

ℓ_U = mean free path for phonon-phonon scattering; and

ℓ_D = mean free path for phonon scattering by defects or impurities.

If the concentration of defects is changed, the mean free path for defect scattering changes to some different value, ℓ'_D, and the resultant mean free path assumes a new value, ℓ'. Equation (3) then becomes

$$\frac{1}{\ell'} = \frac{1}{\ell_B} + \frac{1}{\ell_U} + \frac{1}{\ell'_D} . \tag{4}$$

The ratio of resultant mean free paths, obtained by dividing (3) by (4), is:

$$\frac{\ell'}{\ell} = \frac{1 + A}{\dfrac{\ell_D}{\ell'_D} + A} , \tag{5}$$

where $A = \left(\dfrac{\ell_D}{\ell_U} + \dfrac{\ell_D}{\ell_B} \right) .$ (6)

This of course assumes that only ℓ_D changes while ℓ_B and ℓ_U remain constant. In fact, the constancy of ℓ_U cannot be established, and it is possible that ℓ_U and ℓ_D may not be separable.

It seems likely that the major effect of changing the defect concentration, and thus introducing new scattering centers, is to alter the periodicity of the potential field associated with the graphite structure, which would affect the value of ℓ_U. It appears reasonable, therefore, to rewrite eq. (3) in the form

$$\frac{1}{\ell} = \frac{1}{\ell_B} + \frac{1}{\ell_U} \quad . \tag{7}$$

Now ℓ_U is understood to include effects due to defects and impurities. When these change in concentration ℓ_U changes to ℓ'_U and, dividing as above,

$$\frac{\ell'}{\ell} = \frac{1 + F}{\dfrac{\ell_U}{\ell'_U} + F} \quad , \tag{8}$$

where

$$F = \frac{\ell_U}{\ell_B} \quad , \tag{9}$$

The similarity of equations (5) and (8) is obvious, and this form of the equation is general for any number of variables treated in this way. Whether eq. (3) contains 3 terms, 2 terms, or n terms, the equation relating ℓ' to ℓ is always of the same form, differing only in the terms contained in the constant A (eq. 5) or F (eq. 8).

As defect or impurity concentration increases, ℓ'_U must decrease. The ratio ℓ_U / ℓ'_U must increase in proportion to impurity concentration, and also to total radiation dosage or any other variable which increases defect concentration. If crystallite size (i.e., ℓ_B) is constant, ℓ' must vary with ℓ'_U. Thermal conductivity is given by:

$$\lambda = \frac{1}{3} \sum_{i=1}^{n} C_i V_i \ell \tag{10}$$

where   C = heat capacity,

V = phonon velocity,

i = acoustic mode index.

Since λ varies with ℓ', and therefore ℓ'_U, it must decrease as impurity or defect concentration increases. Differentiation of eq. (8) indicates that the curve of λ vs impurity or defect concentration--or any measure of them, such as radiation exposure--should be concave upward, with a negative slope throughout.

B. Experimental

Data for examining unambiguously the relation between thermal conductivity and impurity or defect concentration are rare, since the requirement that ℓ_B (mean crystallite diameter) be constant makes it necessary that

the measurements be made either on a single specimen or on a group of specimens for which ℓ_B is known to be constant. Further, since graphite is strongly anisotropic, evidence is required that the degree of preferred orientation is constant relative to the direction in which measurements are made.

The boundary conditions of constant ℓ_B and constant degree of preferred orientation were met in a CMF-13 investigation of the effects of small boron additions on the properties of an extruded polycrystalline graphite. The effect of boron on the room-temperature thermal conductivity of this graphite is shown in Fig. 6. The shape of the curve is that predicted above from the simple phonon-scattering model.

Smith and Rasor (Phys. Rev. 104, 885, 1956) reported the effects of neutron irradiation and the formation of bromine residue compounds on the thermal conductivities of graphites. They did not measure ℓ_B or degree of preferred orientation, but did take considerable care to as-
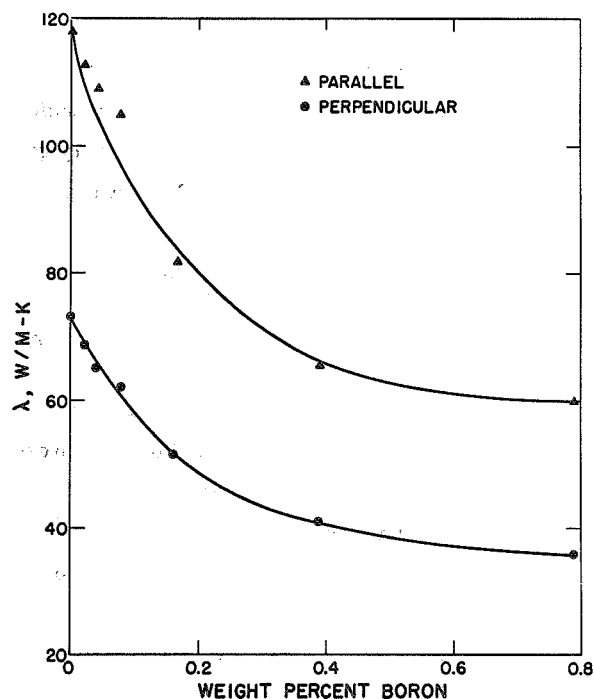

Fig. 6. Effect of boron on the room-temperature thermal conductivity of a polycrystalline graphite. Measurements made parallel and perpendicular to the extrusion axis.
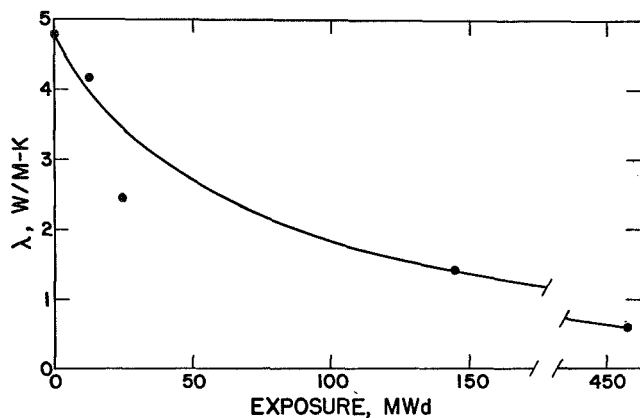
Fig. 7. Effect of neutron irradiation on thermal conduc-
tivity of SA-25 graphite, measured at 100K.
Data of Smith and Rasor. (One megawatt-day
equals 10^7 nvt of neutrons with energies greater
than 0.5 mev.)

Fig. 8. Effect of residual bromine content on the thermal
conductivity of AGOT-KC graphite, measured at
100K. Data of Smith and Rasor.

sure that their measurements were not unduly influenced
by variables other than those intended. Their data are
of particular interest because neutron irradiation pro-
duces severe lattice defects while bromine residue com-
pounds have their greatest effect on the character of the
crystallite boundaries, permitting the effects of ℓ_U and
ℓ_B to be considered more or less independently. Their
results were presented as plots of λ vs temperature,
with total neutron exposure or bromine content as inde-
pendent parameters. Thermal conductivity of SA-25
graphite measured at 100K has been taken from these
curves and replotted in Fig. 7 as a function of total neu-
tron exposure. Again as would be predicted from the
phonon-scattering model, the curve has diminishing neg-
ative slope, and this is true of all of the neutron-irradi-
ation data reported by Smith and Rasor.

Graphite-bromine residue compounds are made by
allowing bromine to react with graphite to form unstable
lamellar compounds, then heating to permit the com-
pounds to decompose. At all but extremely high temper-
atures (> 2000°C) some residual bromine remains in the
crystallite boundaries and other discontinuities of the
graphite structure. This does not change crystallite size
but, with regard to phonon-scattering, has the equivalent
effect of increasing the scattering efficiency of the crys-
tallite boundaries. (This has been discussed by Jamieson
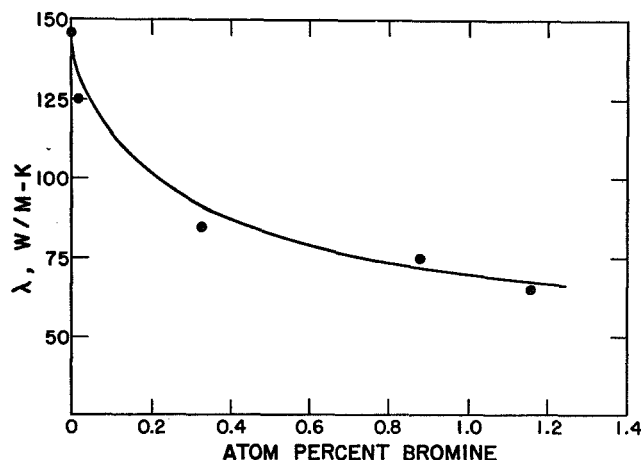and Mrozowski, Proc. Second Carbon Conference, 1956.)

For the AGOT-KC graphite investigated by Smith and
Rasor, it was estimated that a little more than one atomic
percent of residual bromine could be accomodated without
damaging the graphite crystallites themselves. Their
data below this limiting concentration are replotted in
Fig. 8. Again the curve shape is that which would be ex-
pected from phonon scattering, as deduced in this case
from the assumptions that an increase in boundary scat-
tering efficiency is equivalent to a reduction in crystallite
size, and that scattering by defects, other impurities,
and phonon-phonon interactions has not been affected by
the introduction of bromine.

At temperatures well below room temperature ℓ_U
becomes large, and in extreme cases $\ell = \ell_B$. With de-
creasing temperature, then, the ratio ℓ_U / ℓ'_U becomes
very small, ℓ_U / ℓ_B becomes relatively large, and, from
eq. (8), ℓ'/ℓ approaches unity. It would be expected that
thermal conductivity curves for materials differing only
in defect concentration would converge with decreasing
temperature in the cryogenic region of temperatures.
Again, data for investigating this are rare because of the
requirements of constant crystallite size (ℓ_B) and degree
of preferred orientation. However, the work of Powell
and Wagner (Carbon, in press, 1970) seems to meet these
requirements, as do some of Smith and Rasor's data.
Powell and Wagner used specimens made from three com-

25

mercial graphites, and measured thermal conductivity over the temperature interval 20K to about 100K before and after neutron irradiation. Conductivity at 100K was reduced by irradiation to approximately 15% of its original value. However, as is shown in Fig. 9, the curves of λ vs T for the unirradiated and irradiated specimens converged with decreasing temperature, as was predict-ed above. The data of Smith and Rasor on both irradiated and brominated graphite show similar trends, the λ vs T curves for untreated and treated samples tending to
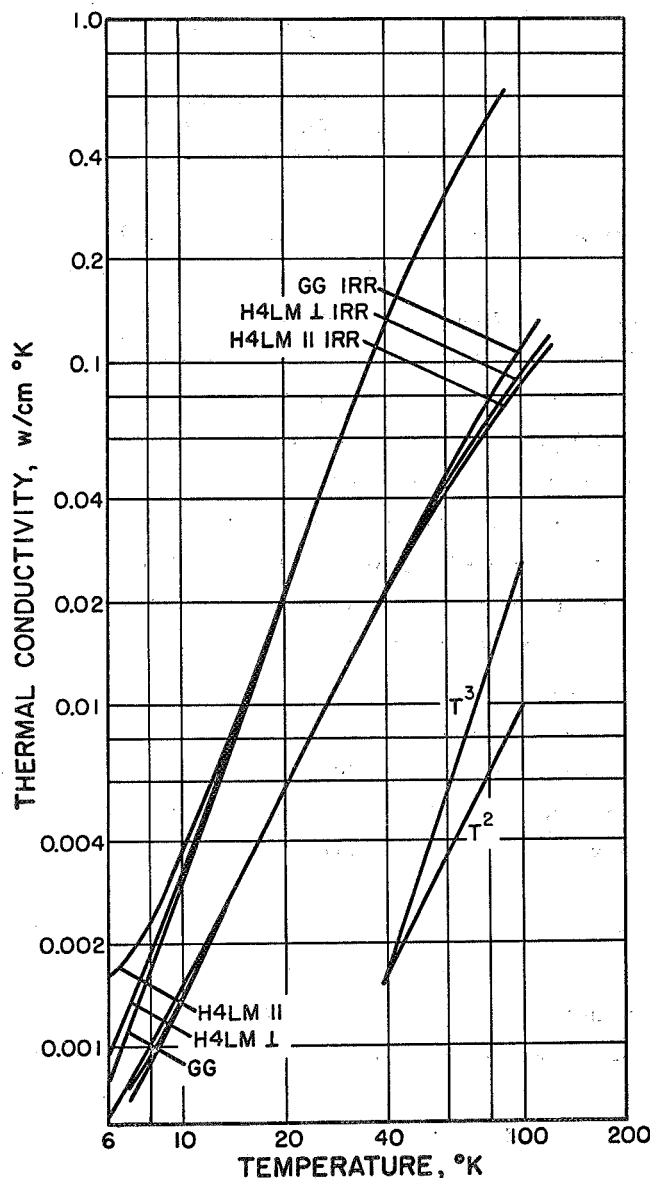
converge as temperature decreased from 300K to 20K. Thus the analysis of low-temperature thermal conduction based on the phonon-scattering model is substantiated experimentally despite the anticipation that, by analogy with electrical properties, some residual thermal resistivity would exist at 0°K.

Ivanov (Teplofizika Vipokikh Temperatur $\underline{4}$, 875, 1966) has suggested that for scattering in porous materials the resultant mean free path should be calculated from an equation similar to eq. (3) except that ℓ_D is replaced by the mean distance between pores. Data are now being generated on CMF-13 graphites having controlled structures, and preliminary results appear to agree with Ivanov's formulation. This further supports the phonon-scattering concept for graphite.

C. Discussion

So far as immediate applications of the phonon-scattering model are concerned, the most important is to multiphase systems. It has been customary to express the thermal conductivity of a multiphase system in either of the following two forms:

$$\lambda = \sum_{i=1}^{n} a_i \lambda_i \tag{11}$$

$$\frac{1}{\lambda} = \sum_{i=1}^{n} \frac{a_i}{\lambda_i} \tag{12}$$

The reasons for using one form instead of the other have not been defined, and both types of expressions appear in the literature. Taking graphite as an extreme case of a multiphase system, the pore structure being the second phase, the results outlined above support the use of eq. (12) for this purpose. Further, since interfacial boundaries act as phonon scatterers in multiphase systems, the fact that eq. (12) applies to multiphase systems in general as well as to graphite supports the view that phonon propagation plays a major role in heat conduction in graphite.

Fig. 9. Effects of irradiation and temperature on the thermal conductivities of H4LM and Graph-i-tite G graphites. Data of Powell and Wagner.

VIII. DIAMETRAL THERMAL EXPANSION
OF COATED FUEL PARTICLES
(W. V. Green, E. G. Zukas, P. Wagner)

Over a period of several months, a number of attempts have been made in CMF-13 to measure directly the diametral thermal expansion of pyrolytic-carbon-coated UC_2 fuel particles. None of the methods tried has been completely satisfactory. However, three sets of results have now been obtained which permit a reasonable estimate to be made of this value.

P. Wagner has used a quartz dilatometer to measure the motion of a quartz piston in contact with the surface of a sample of fuel particles contained in a quartz cylinder, as the sample was heated from 25 to 645°C. The volume change of the container was taken into account, and the measurement reduced to an average linear CTE of the particles over this temperature interval. The output of the transducer which measured piston motion was jagged rather than smooth, which is attributed to intermittent "locking up" of the stacked particles until the stresses developed by further thermal expansion were sufficient to free them again. The two best runs of several trials gave values of 5.5 and 6.2 x 10^{-6}/°C, for an average of 5.85 x 10^{-6}/°C over the temperature interval 25 to 645°C.

W. V. Green and E. G. Zukas have used a travelling microscope to measure the change in length of a column of closely sized fuel particles stacked in the bore of a quartz capillary tube whose inside diameter was slightly larger than the diameters of the particles. Each column consisted of 200 to 300 coated particles. In spite of the care taken in selecting particles and filling the tube, holding the tube in an inclined position, tapping it to rearrange particles, etc., many of the particles formed spiral rather than linear arrangements. No measurable change in length of the columns resulted from cycling between room temperature and 1200°C, so that these arrangements were evidently stable and expansion of the column was reversible. However, because the CTE of quartz is less than that of the particles, heating necessarily caused straightening of the spiral arrays, creating

an increment of column-length change which added to that produced directly by expansion of the particles. In one set of experiments the bore diameter was about 50% greater than the average particle diameter, and--assuming monosize, spherical particles, constant bore diameter, and a spiral particle arrangement throughout the column-- this increment of length change was calculated to be 40% of that produced directly by thermal expansion. In a second set of measurements the bore diameter was about 20% larger than the average particle diameter, and the increment so calculated was 10% of the actual thermal expansion. Since the spiral arrangement appeared not to exist everywhere in the column, these corrections are probably too large.

Over the temperature interval 25 to 1200°C, individual, uncorrected CTE values from the first set of measurements were 8.6, 8.1, 7.7, and 8.6 x 10^{-6}/°C, for an overall average of 8.25 x 10^{-6}/°C. Applying the above correction for column straightening, this reduces to 5.9 x 10^{-6}/°C. Uncorrected values from the second set of measurements were 7.1, 6.8, 5.2, 5.0, and 5.7 x 10^{-6}/°C, for an average of 6.0 x 10^{-6}/°C and a corrected value of 5.5 x 10^{-6}/°C. Total length change of the column from heating over this temperature interval was about 0.2 mm, measurement uncertainty was about 0.02 mm, and the corresponding uncertainty in each CTE determination was therefore about ± 0.6 x 10^{-6}/°C.

It is not obvious how these values should be weighted to determine a probable best value for the diametral CTE of coated fuel particles. Wagner's results, from measurements over a lower temperature interval, should be lower than those of Green and Zukas. They are not, suggesting that the straightening correction made by Green and Zukas was indeed excessive. Somewhat arbitrarily, a preferred value of 5.8 x 10^{-6}/°C has been selected for the temperature interval 25 to 1200°C, with an uncertainty of about ± 0.5 x 10^{-6}/°C.

IX. RAW MATERIALS

A. Santa Maria Cokes (R. D. Reiswig, L. S. Levinson)

New lots of Santa Maria Green Coke and Santa Maria LV (calcined) Coke, identified as CMF-13 Lots CL-8 and CL-9 respectively, have been obtained from Collier Carbon and Chemical Corporation. Microscopically they appear to be identical with the several lots previously obtained.

B. Pitch Residue (L. S. Levinson, R. D. Reiswig)

A sample of Barrett 30 MH coal-tar pitch (CMF-13 Lot PP-3) was dissolved in quinoline and the residue examined in both the as-extracted and the graphitized condition. Both residue samples were dispersed ultrasonically in a 1% Aroplaz-Xylene solution and placed on carbon grids for electron microscopy. The as-extracted material contained individual particles $0.1-0.2\mu$ dia, and clumps of such particles. Some particles were angular and had sharp outlines, but the majority were circular in section and did not have clearly defined edges. Selected-area diffraction patterns from the particles were similar to the background from the carbon grid, indicating that they were nearly amorphous.

After graphitization the material was in the form of lumps which did not disperse well. These were ground in a hand mortar and the fragments dusted on a carbon grid. Selected-area diffraction patterns contained both fairly sharp rings and spots superimposed on the rings. Some of the fragments were small flakes of highly graphitic material, which were probably responsible for the sharp diffraction spots. The rest were aggregates whose basic structural unit could not be determined, which were probably responsible for the diffraction rings. A sample of the fragments was mounted in an epoxy resin, polished and etched, replicated, and the replica examined in the electron microscope. Two types of material were observed: (1) Particles of carbon black, circular in section, with diameters ranging from a few tenths to about 1.5μ. These appeared to have a nucleus and a layered concentric structure. Particles plucked from the sample when the replica was removed produced diffraction rings similar to those from the dusted grid. (2) Lamellar particles, generally long and narrow, containing few if any blacks. These are probably quinoline-soluble pitch which was trapped with the quinoline in the mass of insoluble particles when the quinoline extraction was completed, and then concentrated and redeposited when the trapped solvent was evaporated. These particles are believed not to be properly part of the quinoline-insoluble fraction of the pitch.

The quinoline-insoluble fraction of 30MH pitch appears, then, to consist largely or entirely of carbon black in the particle-size range up to about 1.5μ dia. The appearance in the samples described above of well-graphitized material, apparently derived from the quinoline-soluble fraction, suggests an explanation for the fact that solvent-blended graphites made with 30MH pitch are often observed to contain a few regions which are very rich in carbon black and many regions which contain none. The solvent and the dissolved pitch which it contains apparently separate from the insoluble carbon black during blending. When the solvent subsequently evaporates the soluble pitch is left as a coating on filler particles, where it ultimately graphitizes well and usually cannot be distinguished optically from the filler material. The local concentrations of carbon black produced by this separation are probably an undesirable feature of the structure produced by solvent-blending.

X. PUBLICATIONS RELATING TO CARBONS AND GRAPHITES

Wewerka, E. M. and Dickinson, J. M., "The Use of Differential Thermal Analysis as a Method of Determining Graphite Fabrication Variables", Abstract in: Carbon, Vol. 7. p. 709-710, 1969.

Dickinson, J. M., Armstrong, P. E. and Wagner, P., "Modification of an Isotropic Graphite by Use of Acicular Flour Additions", Abstract in: Carbon, Vol. 7, p. 710, 1969.

Zukas, E. G. and Green, W. V., "Creep Behavior of Hot Isostatically Pressed Graphite", Abstract in:

Carbon, Vol. 7, p. 729, 1969.

Green, W. V. and Zukas, E. G., "Microstructural
Changes Produced in Graphite by High Temperature
Creep", Abstract in: Carbon, Vol. 7, p. 729, 1969.

Reiswig, R. D., Armstrong, P. E. and Levinson, L. S.,
"Thermal Shock Testing using Focused Electron
Beam Heating", Abstract in: Carbon, Vol. 7, p. 732,
1969.

Wagner, P., Dickinson, J. M. and Dauelsberg, L. B.,
"The Effect of Boron on Some Properties of a Poly-
crystalline Graphite", Abstract in: Carbon, Vol. 7,
p. 735, 1969.

Smith, M. C., "CMF-13 Research on Carbon and Graph-
ite, Report No. 12, Summary of Progress from
November 1, 1969 to January 31, 1970", LASL Re-
port No. LA-4417-MS, April, 1970.

Green, W. V. and Zukas, E. G., "Stored Energy in
Creep Deformed Graphite", Nature, Vol. 225, p.
628-629, 1970.

Levinson, L. S., Reiswig, R. D. and Baker, T. D., "An
Observation on the 'Lamellar' and 'Scaly' Microstruc-
ture of Graphite", Letter-to-the-Editor in: Carbon,
Vol. 8, No. 1, 1970.

Wagner, P., "Equipment and Techniques for Measure-
ments of Thermal Conductivity, Thermal Expansion
and Associated Properties above 1000°C", Proc.
European Conf. on Thermophysical Props. of Solids
at High Temps., Baden-Baden, 1968, Report No.
BMBW-FB K 70-01, p. 145-175, February, 1970.

Reiswig, R. D., Wewerka, E. M., Levinson, L. S. and
O'Rourke, J. A., "On the Origin of Coke Micro-
structures", Letter-to-the-Editor in: Carbon, Vol.
8, No. 2, p. 241-242, 1970.